

**Coherent Optical Signal Processing for a Doppler Lidar using a
Michelson Interferometer**

R. L. Schwiesow and S. D. Mayor

National Center for Atmospheric Research, ATD/RSF

PO Box 3000, Boulder, CO 80307-3000, USA

phone: 303-497-2061, internet: schwies@ncar.ucar.edu

Small changes in optical wavelength can be measured with a Michelson interferometer. We show how multiple optical delays allow practical Doppler measurements at short wavelengths.

Reprinted from:

Coherent Laser Radar, Vol. 19, OSA Technical Digest Series

(Optical Society of America, Washington DC, 1995), pp. 212-215.

Coherent Optical Signal Processing for a Doppler Lidar using a Michelson Interferometer

R. L. Schwiesow and S. D. Mayor

National Center for Atmospheric Research, ATD/RSF
PO Box 3000, Boulder, CO 80307-3000, USA
phone: 303-497-2061, internet: schwies@ncar.ucar.edu

1. Background

There are a number of reasons to consider operating a Doppler lidar at wavelengths near $1 \mu\text{m}$ rather than at $10.6 \mu\text{m}$. A very important one for NCAR applications is that the shorter-wavelength lidar offers better range and velocity resolution for measurements in the turbulent boundary layer because the product of range resolution and spectral width of the velocity spectrum is proportional to the wavelength. In addition, the quantized backscattering coefficient (number of photons backscattered for a given transmitted pulse energy) may be greater near $1 \mu\text{m}$ than at $10.6 \mu\text{m}$ for particle size distributions with a relatively small mean particle size.

On the other hand, there are a number of difficulties in operating at the shorter wavelength. With optical heterodyne detection, the beat frequencies are high enough ($\approx 2 \text{ MHz per } 1 \text{ m s}^{-1}$ near a wavelength of $1 \mu\text{m}$) to require expensive A/D converters and extremely high data rates for digital processing. Inhomogeneities in atmospheric refractive index limit the effective aperture of lidar telescopes for heterodyning. Eye safety is a concern, and at wavelengths long enough for eye safety (around $2 \mu\text{m}$), reliable laser sources and detectors with good quantum efficiency have been difficult to obtain. As a result, there has been a lively debate in the literature^{1,2} and at previous Coherent Laser Radar Conferences about the relative merits of operation at various wavelengths for various applications.

Research on Doppler lidars at wavelengths near $2 \mu\text{m}$ has been reported using optical heterodyne detection^{3,4}. Because of difficulties with optical heterodyning in this spectral region, Doppler lidars at $0.5 \mu\text{m}$ and shorter wavelengths have been based on signal processing using narrow transmission filters (the "edge" technique)⁵ or using configurations of Fabry-Perot interferometers including either scanning^{6,7}, multiple fixed etalons⁸, or displaced ring patterns with a spatially extended scattering source^{9,10}. The need for Doppler lidar techniques making more efficient use of photons with relatively simple hardware has encouraged us to examine a technique for processing returns from a Doppler lidar by using direct, coherent optical processing rather than high-finesse filters or optical heterodyne detection. This approach attempts to obtain the benefits of lidar operation at shorter wavelengths while avoiding the problems and limitations associated with heterodyning at these wavelengths and those associated with using optical filters or a Fabry-Perot interferometer.

2. Coherent optical measurement of the temporal autocovariance function

A popular technique for processing the signal from heterodyne lidars at $10.6 \mu\text{m}$ involves digitization of the beat-frequency time series from the detector and measurement of the beat frequency (usually around 10 MHz or so) of short segments of the time series by performing a single- or multiple-lag complex autocovariance on each segment. What we analyze in this summary is using elements of the autocovariance of the optical signal directly, without mixing with a local oscillator. Advantages include optical and analytical simplicity and less sensitivity to inhomogeneities in refractive index. The time delay for the optical computation of an autocovariance is provided by the difference in path lengths in the two arms of a Michelson interferometer rather than by the time difference between successive samples of the analog-to-digital (A/D) converter in the digital calculation.

Light from the two paths in a Michelson interferometer, when recombined, will add constructively or destructively, depending on the relative phase of the two beams at recombination. The power detected at the output of the interferometer as a function of optical path difference d is

$$P(d, \lambda) = A[1 + E(d) \cos(2\pi d/\lambda)], \quad (1)$$

where A is some amplitude factor, depending on range and atmospheric scattering, and $E(d)$ is an envelope function, which depends on the spectral width of the components in the input spectrum and shows how fast the interference decays with increasing path difference. Figure 1 is a schematic representation of a typical optical autocovariance function. The autocovariance and the envelope function have been discussed in more detail for a temperature lidar¹¹.

For measuring small shifts of wavelength related to Doppler scattering, we calculate the derivative of $P(d, \lambda)$ with respect to λ with d fixed to obtain

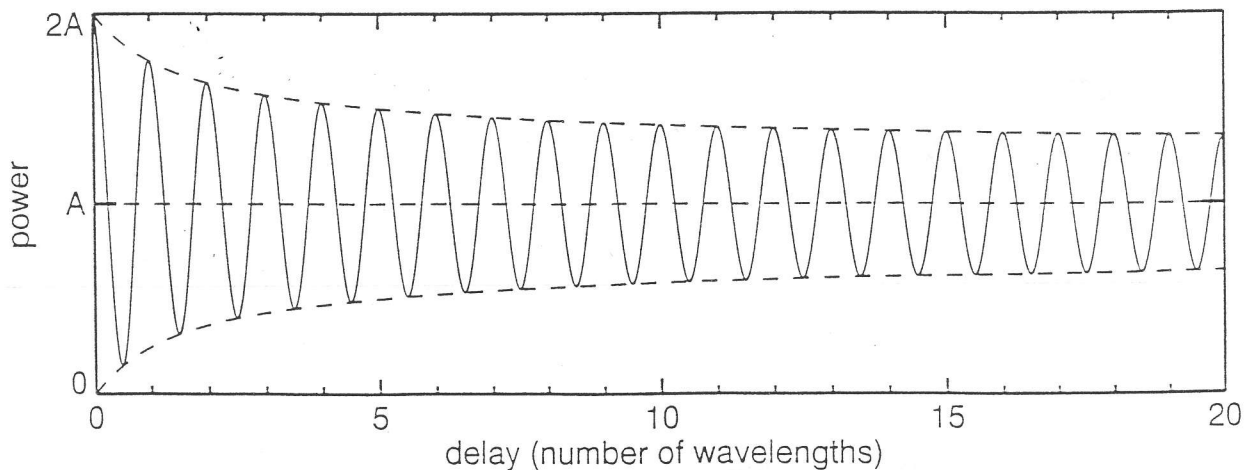


Fig. 1. Schematic representation of an optical autocovariance function.

$$\partial P/\partial \lambda = A[E(d) 2\pi d/\lambda^2] \sin(2\pi d/\lambda). \quad (2)$$

This is relatively largest when the $|\sin|$ factor is near one, i.e., when $2\pi d/\lambda$ is some odd integer times $\pi/2$. The change in power for a given change in wavelength increases with increasing delay, so one can choose the spectral resolution by choosing optical delay d . To visualize the effect of changing λ slightly, imagine the oscillatory trace in fig. 1 stretching or shrinking like a spring, with the left end fixed.

3. Application to Doppler signals

To estimate the required d for typical Doppler signals, consider a velocity range of $\pm 20 \text{ m s}^{-1}$ for which a normalized change in power of ± 0.5 is chosen to occur. Substituting $\Delta\lambda$ from the Doppler equation in the finite-difference form of eqn (2) gives a value $d_0 = 0.63 \text{ m}$ for the assumed conditions. This is about 6×10^5 fringes. With a normal folded path, the major physical dimension of the interferometer is just over $d_0/2$, which is a reasonable size for a fieldable lidar instrument. The sensitivity of the measurement to velocity changes can be increased by increasing d_0 , which in turn leads to a reduced full-scale range. In this way, the coherent optical autocovariance technique can be adapted to a wide variety of Doppler lidar applications.

In practice, the autocovariance function of the type in fig. 1 will change with time both in amplitude ($1/\text{range}^2$ and changes in backscatter coefficient) and in delay period (velocity). The signal-processing task is to determine the shift in wavelength $\Delta\lambda(t)$ for successive time periods averaged over approximately 100 ns (15-m range gate length) each. From eqn (2), we note that there are three unknowns [$\Delta P(t)$, $A(t)$, and $E(d,t)$] to determine the Doppler shift $\Delta\lambda(t)$. This requires three measurements, as outlined below.

4. Implementation of the coherent optical measurement of Doppler shift

To determine the variables in eqn (2), we make power measurements (at each range gate) at three different, but closely spaced, optical delays near the d_0 calculated above. Figure 2 illustrates a typical measurement with delays d_1 , d_2 , and d_3 set at successive intervals of $\lambda/4$ in total path difference. Sensitivity is best if at time $t = 0$ (for the transmitted wavelength) signals $S_1(0)$ and $S_3(0)$ are nearly equal, i.e., at zero-crossings of the sine wave. This can be arranged by making fine adjustments to the delay with a piezo-electric translator (PZT). In this way, the interferometer tracks changes in the laser transmitter wavelength. Figure 2 shows a portion of the autocovariance function at some later time t where the return has been Doppler shifted.

Although the three measurements can be fit to eqn (2) in a least squares sense, it is instructive to note approximate solutions. For example, $A(t)$ is simply $[S_1(t) + S_3(t)]/2$. In the limit $\Delta\lambda = 0$, $E(d,t) = A(t) - S_2(t)$. Otherwise, $E(d,t)$ is obtained from the fitting procedure. It is possible to obtain the three delays in a single interferometer structure by dividing the collimated beam into three segments, making essentially three stacked interferometers, or by using polarization division, for example.

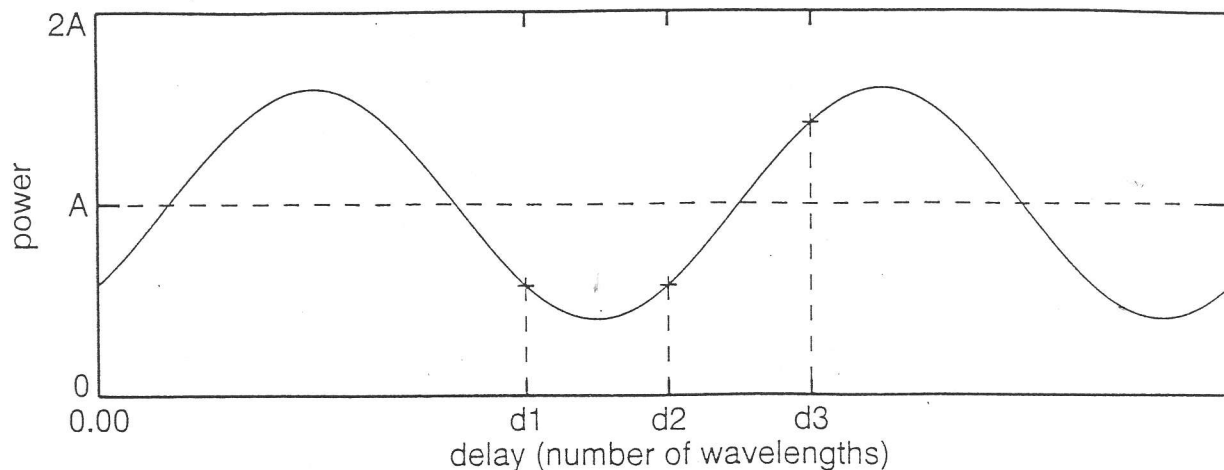


Fig. 2. Schematic view of the optical autocovariance function measured at three closely spaced delays, d_1 , d_2 , and d_3 at some time t after the laser pulse. Corresponding signal levels are $S_1(t)$, $S_2(t)$, and $S_3(t)$.

In the first instance, the interferometer would use a stepped mirror with differences in step heights of $\lambda/8$, which can be obtained with normal thin-film techniques. In the second, relative delay differences of $\lambda/4$ between orthogonally polarized components are introduced with ordinary quarter-wave plates.

5. References

1. R.T. Menzies, "Doppler lidar atmospheric wind sensors: a comparative performance evaluation for global measurement applications from earth orbit," *Appl. Opt.* **25**, 2546-2553 (1986).
2. T.J. Kane, B. Zhou and R.L. Byer, "Potential for coherent Doppler wind velocity lidar using neodymium lasers," *Appl Opt.* **23**, 2477-2581 (1984).
3. S.W. Henderson, P.J.M. Suni, C.P. Hale, S.M. Hannon J.R. Magee, D.L. Bruns and E.H. Yuen. "Coherent laser radar at $2 \mu\text{m}$ using solid-state lasers," *IEEE Trans. Geo. Remote Sensing* **31**, 4-15 (1993).
4. C.J. Grund, "The NOAA $2 \mu\text{m}$ coherent Doppler lidar," *Optical Remote Sensing of the Atmosphere, 1995 Technical Digest Series Volume 2* (Optical Society of America, Washington, DC) 62-64 (1995).
5. B.M. Gentry and C.L. Korb, "Edge technique for high-accuracy Doppler velocimetry," *Appl. Opt.* **33**, 5770-5777 (1994).
6. G. Benedetti-Michangeli, F. Congeduti and G. Fiocco, "Measurement of aerosol motion and wind velocity in the lower troposphere by Doppler optical radar," *J. Atmos. Sci.* **29**, 906-910 (1972).
7. C.A. Tepley, S.I. Sargoytchev and R. Rojas, "The Doppler Rayleigh lidar system at Arecibo," *IEEE Trans. Geo. Remote Sensing* **31**, 36-47 (1993).
8. M.L. Chanin, A. Garnier, A. Hauchecorne and J. Porteneuve, "A Doppler lidar for measuring winds in the middle atmosphere," *Geophys. Res. Lett.* **16**, 1273-1276 (1989).
9. V.J. Abreu, T.L. Killeen and P.B. Hays, "Tristatic high resolution Doppler lidar to study winds and turbulence in the troposphere," *Appl Opt.* **20**, 2196-2202 (1981).
10. J. Sroga and A. Rosenberg, "0.53 μm incoherent Doppler lidar: current status," *Topical Meeting on Laser and Optical Remote Sensing, Technical Digest Series Volume 18* (Optical Society of America, Washington, DC) 320-323 (1987).
11. R.L. Schwiesow and L. Lading, "Temperature profiling by Rayleigh-scattering lidar," *Appl. Opt.* **20**, 1972-1979 (1981).